

Supporting Information for

Evolution of surface and sub-surface morphology and chemical state of exsolved Ni nanoparticles

Heath Kersell,^{1,*} Moritz L. Weber,^{2,3} Lorenz Falling,¹ Qiyang Lu,^{1,†} Christoph Baeumer,⁴ Nozomi Shirato⁵
Volker Rose,^{5,6} Christian Lenser,³ Felix Gunkel,² Slavomír Nemsák^{1,*}

¹Advanced Light Source, Lawrence Berkeley National Laboratory, Berkeley, California, 94720, United States

²Peter Gruenberg Institute (PGI-7) and JARA-FIT, Forschungszentrum Jülich GmbH, 52425 Jülich, Germany

³Institute of Energy and Climate Research (IEK-1), Forschungszentrum Jülich GmbH, 52425 Jülich, Germany

⁴MESA+ Institute for Nanotechnology, University of Twente, Faculty of Science and Technology, 7500 AE Enschede, The Netherlands

⁵Center for Nanoscale Materials, Argonne National Laboratory, Lemont, Illinois 60439, United States

⁶X-ray Science Division, Advanced Photon Source, Argonne National Laboratory, Lemont, Illinois 60439 United States

1. Fitting for the Ni 3p and Ti 3s Regions

Fig. S1 shows fits for the Ni 3p and Ti 3s regions at 900 eV photon energy on STNNi after reducing in 1 Torr H₂ at increasing annealing times and temperatures. Fits for Ni²⁺, Ni⁰, and Ti⁴⁺ components are shown in red, blue, and black, respectively. All Ni 3p species (Ni²⁺ and Ni⁰) are fitted with Voigt type doublets, having fixed spin orbit splitting, branching ratios, and widths. Meanwhile, the Ti 3s region is fit with a singlet. Full width at half maxima (FWHM) are fixed for each species across all conditions. Binding energies are calibrated as discussed in section 2 of the main text.

2. Elemental Identification of STNNi Features

In Figure 3 of the main text, we show AFM imaging of an STNNi surface before and after reducing treatment. Before the reducing treatment, the surface is bare, consisting only of STNNi steps. After reducing in H₂ gas at 800 °C, the surface is decorated by high contrast structures averaging 27.8 nm wide and 7.1 nm high. The reduced surface also contains low contrast features with a height of just 0.4 nm (main text, Fig. 3b, inset). The three-dimensional morphology of the brighter features is consistent with nanoparticle formation upon Ni exsolution^{[1][2]}, while the 0.4 nm height of the low contrast features is consistent with the height of one SrTiO₃ unit cell. This suggests that the latter features are related to a relaxation or reconstruction of the STNNi host lattice during the reduction and nanoparticle formation.

To support the identification of the features observed in AFM, we also measured X-ray absorption spectroscopy (XAS) using SX-STM to locally probe the surface composition.^{[3][4]} As stated in the main text, the Ni L₃-edge intensity was measured every 12 nm in a 216 nm × 300 nm region (450 total positions) to enable detection of the features with approximately 27 nm width on our surfaces. Fig. S2a shows the L₃-edge intensity at each of the 450 points measured, with three locations having significantly higher Ni intensity than others. These intensities are also plotted as a 216 nm × 300 nm 2D map in Fig. S2b, where

* Corresponding authors: hkersell@lbl.gov, snemsak@lbl.gov

†Current address: Key Laboratory of 3D Micro/Nano Fabrication and Characterization of Zhejiang Province, School of Engineering, Westlake University, Hangzhou, Zhejiang, China.

three bright green pixels appear at the locations with high Ni intensity. To check whether this agrees with the distribution of features in the AFM images, we counted the number of both high and low contrast features in thirty different $216 \text{ nm} \times 300 \text{ nm}$ regions on pre-exsolved samples. Approximately 4.9 ± 1.3 high contrast features and 14.8 ± 2.6 low contrast features appeared in each region (where 1.3 and 2.6 are the respective standard deviations). The appearance of three locations with high Ni intensity is consistent with the distribution of high contrast features on the pre-exsolved samples. This is in agreement with the attribution of the high contrast features as exsolved Ni nanoparticles. We caution that finer resolution should be used in order to conclusively identify the high contrast features as Ni nanoparticles. Finer resolution in future SXSTM measurements on exsolved nanoparticles can be obtained by simply decreasing the distance between measurement points. Nevertheless, because the high contrast features are observed in AFM upon Ni migration, in response to reducing treatments, this further supports the identification of the high contrast features as Ni particles. Meanwhile, the 0.4 nm height of the low contrast features observed in AFM suggests a possible relationship to the STO host surface.

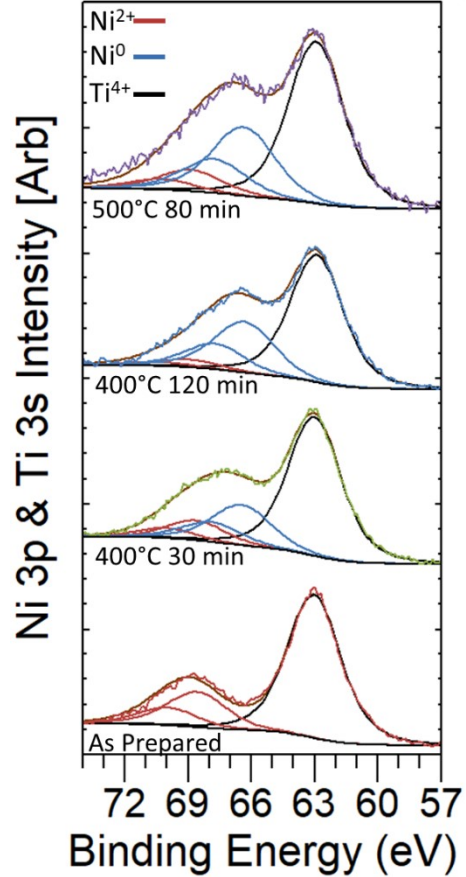


Fig. S1: Ni 3p and Ti 3s regions at 900 eV photon energy are shown on STNNi before reducing treatments, and then after reducing in 1 Torr H_2 at increasing annealing times and temperatures. Fits for Ni^{2+} , Ni^0 , and Ti^{4+} components are shown in red, blue, and black, respectively.

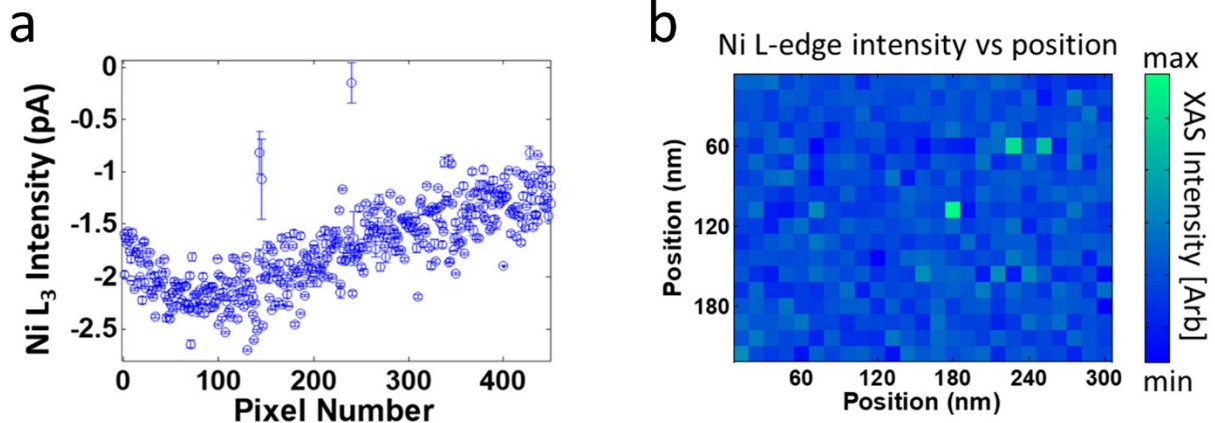


Fig. S2. Ni L_3 -edge intensity measured at 12 nm intervals on STNNi is shown in (a). Measurements in (a) were recorded over a $216 \text{ nm} \times 300 \text{ nm}$ region, shown in (b) with relative XAS intensity plotted at each point.

References

- [1] M. L. Weber, M. Wilhelm, L. Jin, R. Dittmann, R. Waser, O. Guillon, C. Lenser and F. Gunkel, "Exsolution of Embedded Nanoparticles in Defect Engineered Perovskite Layers," *ACS Nano*, 15, 3, 4546-4560, 2021.
- [2] K. J. Kim, H. Han, T. Defferriere, D. Yoon, S. Na, S. J. Kim, A. M. Dayaghi, J. Son, T.-S. Oh, H. M. Jang and G. M. Choi, "Facet-Dependent in Situ Growth of Nanoparticles in Epitaxial Thin Films: The Role of Interfacial Energy," *J. Am. Chem. Soc.*, 141, 7509-7517, 2019.
- [3] H. Kersell, N. Shirato, M. Cummings, H. Chang, D. Miller, D. Rosenmann, S.-W. Hla and V. Rose, "Detecting element specific electrons from a single cobalt nanocluster with synchrotron x-ray scanning tunneling microscopy," *Appl. Phys. Lett.*, 111, 103102, 2017.
- [4] N. Shirato, M. Cummings, H. Kersell, Y. Li, B. Stripe, D. Rosenmann, S.-W. Hla and V. Rose, "Elemental Fingerprinting of Materials with Sensitivity at the Atomic Limit," *Nano Lett.*, 14, 11, 6499-6504, 2014.